

## Thermal Dehydration of Nafagrel Hydrochloride Hydrate at Controlled Water Vapor Partial Pressures

Hiroaki KITAOKA,\* Kazumi OHYA, and Hideo HAKUSUI

Developmental Research Laboratories, Daiichi Pharmaceutical Co., Ltd., 16-13 Kitakasai 1-chome, Edogawa-ku, Tokyo 134, Japan. Received March 3, 1995; accepted June 7, 1995

Nafagrel hydrochloride exists as both a hemihydrate and monohydrate. Conversion from the hemihydrate to the monohydrate is not reversible, and both hydrates can coexist in stable equilibrium between 23% relative humidity (RH) and 64% RH. In order to clarify the dehydration behavior, the kinetics of the thermal dehydration of the hydrates was studied by means of isothermal gravimetry at atmospheric pressure with a controlled water vapor pressure. This revealed that dehydration did not depend on absolute humidity but on RH. The dehydration of the hemihydrate proceeded by two-dimensional growth of the nuclei,  $A_2$ , but the mechanism of monohydrate dehydration changed from  $A_2$  to a two-dimensional phase boundary,  $R_2$ , with an increase in RH. The dehydration of the monohydrate proceeded by  $R_2$ , resulting in the production of the hemihydrate at 6.5% RH or above. These kinetic analyses showed that the monohydrate dehydrated faster than the hemihydrate.

**Key words** nafagrel; crystal water; dehydration; isothermal thermogravimetry; activation energy; humidity

Nafagrel ((±)-6-(1-imidazolylmethyl)-5,6,7,8-tetrahydronaphthalene-2-carboxylic acid) hydrochloride is a thromboxane  $A_2$  synthetase inhibitor.<sup>1)</sup> Nafagrel hydrochloride has two stable pseudopolymorphs, nafagrel hydrochloride hemihydrate and nafagrel hydrochloride monohydrate. It is well known that dehydration behavior depends on the external pressure of water vapor, and therefore several studies have dealt with dehydration at various partial pressures of water vapor.<sup>2)</sup>

Our previous paper reported that, under a nitrogen gas flow, the dehydration mechanism of the two nafagrel hydrochloride hydrates changed with the progress of the reaction, and that, under a self-generated atmosphere, the dehydration followed one kinetic mechanism (the hemihydrate,  $A_2$ ; the monohydrate,  $A_3$ ).<sup>3)</sup> This observation implies that the dehydration mechanism could depend on the external pressure of water vapor. We were interested in the kinetic and mechanistic study of the dehydration

behavior of this drug at various humidities. However, no commercial thermal analysis instruments were available for examining the dehydration behavior at controlled partial pressure of water vapor.

A constant humidity generator has recently been developed, and a thermogravimeter has been combined with this generator. This technical progress has enabled us to clarify the dehydration process at controlled partial pressures of water vapor.

The objectives of the present work were to examine in more detail the dehydration behavior of nafagrel hydrochloride hydrates and their interconversion, using a thermogravimeter combined with a constant humidity generator.

### Experimental

**Materials** Nafagrel hydrochloride hemihydrate ( $C_{15}H_{16}N_2O_2 \cdot HCl \cdot 1/2H_2O$ : 301.77) and its monohydrate ( $C_{15}H_{16}N_2O_2 \cdot HCl \cdot H_2O$ :

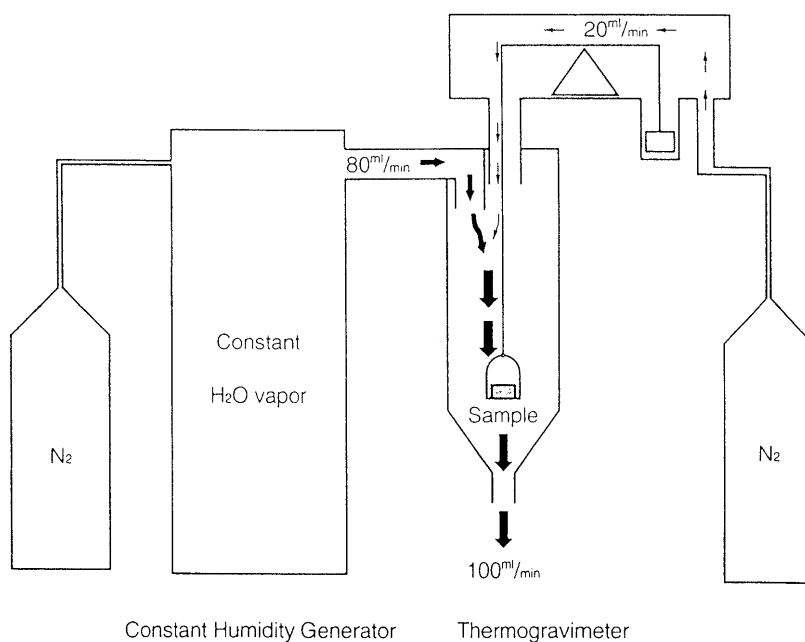


Chart 1. Block Diagram of Thermogravimeter with Constant Humidity Generator

\* To whom correspondence should be addressed.

310.78) of pharmaceutical grade were synthesized in our laboratory. The samples were ground in an agate mortar before use.

**Isothermal Dehydration** Isothermal dehydration was then performed with a Shimadzu TGA-50 thermogravimetric analyzer. The temperature of the furnace was controlled at a temperature between 55 and 65 °C so that it remained within  $\pm 0.5$  °C of that temperature until the dehydration was complete. Sample weights of approximately 5 mg were used, the atmosphere was of nitrogen gas or nitrogen gas containing a constant water vapor content, and a flow rate of 100 ml/min was maintained.

**Control of Water Vapor Partial Pressure** Thermogravimetry was carried out at atmospheric pressure at a controlled water vapor partial pressure of 0–22.5 Torr. Chart 1 is a block diagram of the thermogravimeter used. A Yamato constant humidity generator AHC-1 was employed to generate constant water vapor content. The water vapor partial pressure was controlled as follows: nitrogen gas with a constant water vapor content was passed at a flow rate of 80 ml/min from the constant humidity generator to the thermogravimetric analyzer through a line heated to prevent condensation of the water. The wet nitrogen gas was then mixed with dry nitrogen gas at a flow rate of 20 ml/min to protect the balance against humidity. The final water vapor partial pressures were 0, 4.8, 9.5, 11.4, 14.3, 17.8 and 22.5 Torr.

**Moisture Absorption Equilibrium** Accurately weighed amounts of the hemihydrate and monohydrate were stored in desiccators over phosphorus pentoxide or various saturated salt solutions at 25 and 47 °C (Taiyo Incubator M-230) to give relative humidities (RH) of 0, 11, 23, 33, 43, 52, 64, 75, 83, 93% and 0, 11, 23, 29, 39, 50, 61, 75, 79, 90%, respectively. Weight changes were monitored until constant weights were obtained.

**Powder X-Ray Diffraction Patterns** The powder X-ray diffraction patterns of the samples were obtained using a Mac Science Model MXP-3V diffractometer. The operating conditions were as follows: target, Cu; filter, Ni; voltage, 40 kV; current, 35 mA; receiving slit, 0.15 mm; time constant, 1 s; and scanning speed, 2° 2 $\theta$ /min. Powder X-ray diffractometry at a high temperature was carried out using the same

diffractometer equipped with a Mac Science temperature attachment and controller. After measuring the diffraction at room temperature, the temperature was raised to 40 °C at a heating rate of 10 °C/min, and then the temperature was raised to 50, 55, 60, 65 and 70 °C. Each appointed temperature was maintained for 25 min.

**Measurement of Water Content** The water content of the samples was determined by the Karl Fischer method (type MK-II, Kyoto Denshi Kogyo).

**Infrared (IR) Spectrometry** IR spectra were measured by the KBr disk method using a JEOL JIR-5300 FTIR spectrometer.

## Results and Discussion

**Identification of Pseudopolymorphs** The results of elemental analysis and water content for the pseudopolymorphs are shown in Table 1. The observed values in elemental analysis and water content coincided with the theoretical values, as shown in Table 1.

The powder X-ray diffraction patterns of the anhydrate, the hemihydrate and the monohydrate are shown in Fig. 1. The powder X-ray diffraction patterns of the pseudopolymorphs showed different patterns. Characteristic diffraction peaks were observed at  $2\theta = 6.3, 21.3, 25.5, 31.7^\circ$  for the anhydrate,  $2\theta = 16.8, 24.3, 25.2^\circ$  for the hemihydrate and  $2\theta = 24.7, 27.3^\circ$  for the monohydrate, respectively.

The infrared (IR) spectra of the three forms are shown in Fig. 2. These spectral patterns are different from each other. Especially, there were significant differences among these modifications in the absorption bands due to hydroxyl groups: the monohydrate showed strong absorption bands (at 3515 and 3439  $\text{cm}^{-1}$ ) due to the hydroxyl group in the water of crystallization, while those of the hemihydrate (at 3515 and 3454  $\text{cm}^{-1}$ ) were broad and medium. On the other hand, no absorption band of the anhydrate was observed.

**Moisture Absorption Equilibrium** Figure 3 shows the water content of the hemihydrate and monohydrate after storage at various RH at 25 and 47 °C until constant weights were reached. As shown in Fig. 3, the moisture absorption equilibrium behavior at 47 °C is similar to that at 25 °C. The weight changes were complete within a month, and no further significant changes were detected after storage for 410 d. The hemihydrate was stable between 23 and 64% RH, but dehydration occurred below 23% RH, when an anhydrate was formed. Moisture ab-

Table 1. Elemental Analysis and Water Content of the Pseudopolymorphs

Pseudopolymorph	Elemental analysis (%)				Water content (%)
	Found (Calcd)				
	C	H	Cl	N	Found (Calcd)
Monohydrate	58.01	6.18	11.62	9.05	5.68
	(57.97)	6.16	11.40	9.01	(5.80)
Hemihydrate	59.93	6.00	11.46	9.27	2.98
	(59.70)	6.01	11.75	9.28)	(2.90)
Anhydrate	61.50	5.89	11.91	9.59	—
	(61.54)	5.85	12.11	9.57)	—

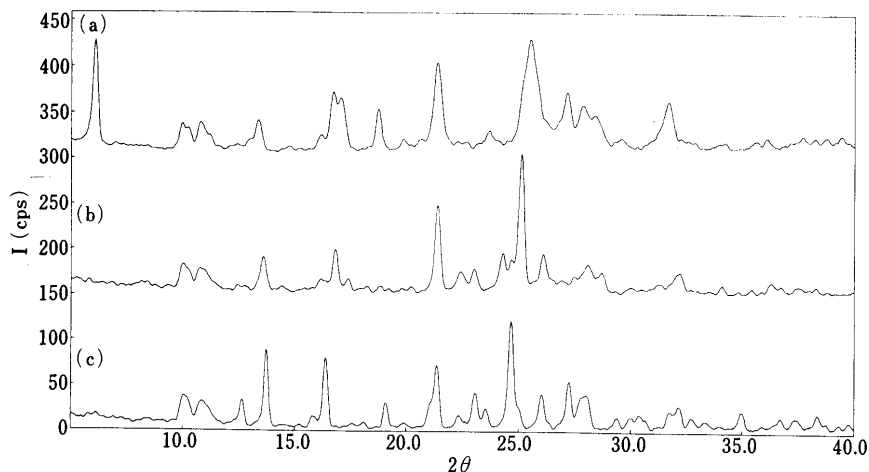


Fig. 1. Powder X-Ray Diffraction Patterns of Nafagrel Hydrochloride Pseudopolymorphs

(a) anhydrate; (b) hemihydrate; (c) monohydrate.

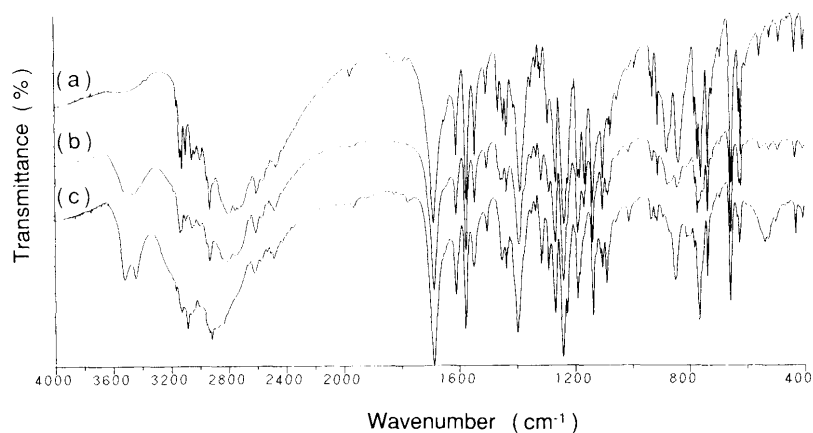


Fig. 2. IR Spectra of Nafagrel Hydrochloride Pseudopolymorphs

(a) anhydrate; (b) hemihydrate; (c) monohydrate.

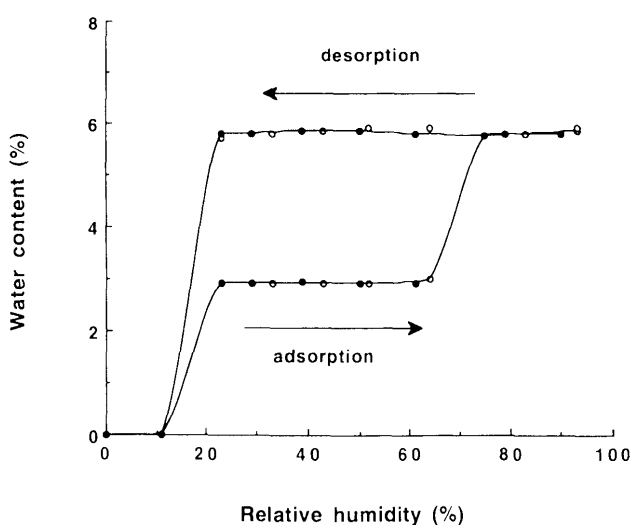


Fig. 3. Moisture Absorption Equilibrium of Nafagrel Hydrochloride at 25 (○) and 47 (●) °C

sorption occurred over 75% RH, resulting in conversion to the monohydrate.

On the other hand, no dehydration of the monohydrate was seen between 23% RH and 64% RH, no conversion into the hemihydrate occurred, and, as in the case of the hemihydrate, no weight loss took place until 11% RH. Neither the hemihydrate nor the monohydrate underwent interconversion between 23% RH and 64% RH. This observation is contrary to the phase rule, and some reports have tried to explain it.<sup>4)</sup> However, we do not think that sufficient explanation for this has been made, and we suggest that the cause may be different for each compound. Therefore, we considered that this observation can be better explained if the dehydration behavior under controlled water vapor partial pressure is examined more closely. We thus carried out a kinetic study of the dehydration of these hydrates using a TG method at controlled water vapor partial pressures corresponding to 0—ca. 15% RH.

**Thermogravimetric Results** Figure 4 shows the isothermal dehydration of the hemihydrate and monohydrate at 60 °C at 0% RH and 12% RH. The observed weight losses of the hemihydrate and the monohydrate coincided with theoretical values for the dehydration of 1/2 mol of water

per mol of the drug (Calcd 2.98%) and 1 mol of water (Calcd 5.80%), respectively. At 0% RH, the dehydration of the hemihydrate took about 15 min and that of the monohydrate was faster, taking about 12 min; by contrast, at 12% RH, the positions were reversed. However, the dehydration trace of the hemihydrate was superposed exactly upon that part of the trace of the monohydrate after half of the water of crystallization had been removed. The same results were observed in the traces made of the monohydrate obtained above 6.5% RH. This suggested that the dehydration of the monohydrate at humidities above 6.5% RH consisted of two steps, the first being dehydration of the monohydrate to hemihydrate, and the second, dehydration of the hemihydrate. Therefore, kinetic analyses of the dehydration were performed using the initial half of the dehydration for monohydrate above 6.5% RH.

**Powder X-Ray Diffraction Analysis** Changes in the powder X-ray diffraction patterns of the hemihydrate and the monohydrate by heating are shown in Figs. 5 and 6, respectively. As seen in Figs. 5 and 6, the powder X-ray diffraction patterns of the hemihydrate and the monohydrate varied with temperature. The samples after heating above 70 °C were confirmed to be anhydrites by determination of their water content using the Karl Fisher method. Figure 6 shows the characteristic peaks ( $2\theta = 16.8, 24.3$  and  $25.2^\circ$ ) of the hemihydrate, and supports that the monohydrate forms the hemihydrate by dehydration under a self-generated atmosphere as reported previously.<sup>3)</sup>

**Kinetics and Mechanisms** The kinetics of solid-state reactions can be represented by the general equation

$$g(\alpha) = kt \quad (1)$$

where  $g(\alpha)$  is a function depending on the reaction mechanism,  $\alpha$  is the fraction of the reaction,  $k$  is the rate constant, and  $t$  is time. Many theoretical model functions have been proposed for  $g(\alpha)$ .<sup>5)</sup> The kinetic mechanisms of the present dehydrations, *i.e.* the model function, were judged on the basis of the linearity of the plots of the  $g(\alpha)$  functions calculated from  $\alpha$  against time for the dehydration, in accordance with Eq. 1. Figures 7 and 8 show  $g(\alpha)$  versus  $t$  plots at 0% RH and 12% RH for the hemihydrate and the monohydrate. Table 2 shows the

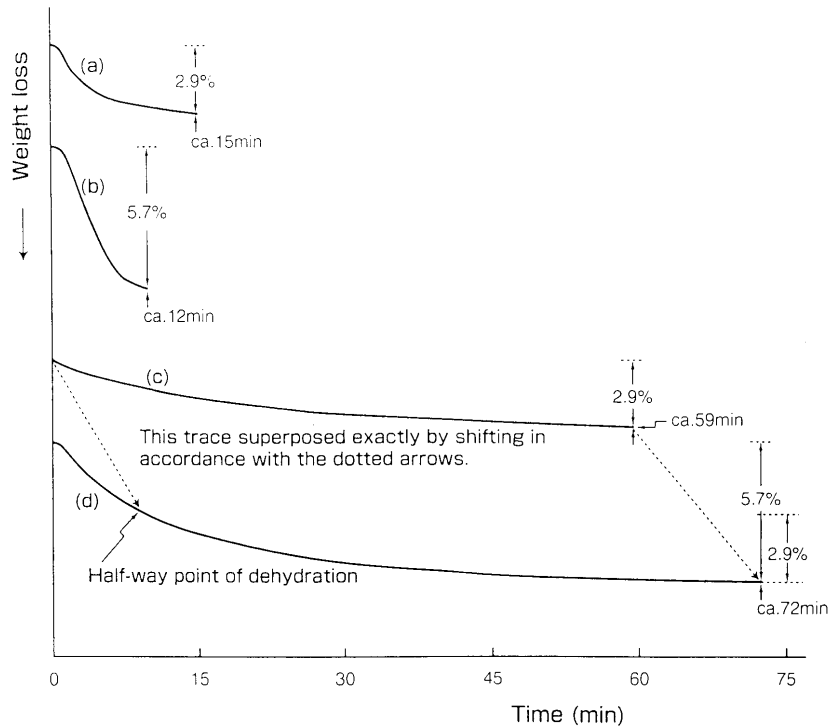


Fig. 4. Isothermal Dehydration of Nafagrel Hydrochloride Hemihydrate and Monohydrate at 60°C  
 (a) hemihydrate at 0% RH (dry nitrogen); (b) monohydrate at 0% RH (dry nitrogen); (c) hemihydrate at about 12% RH; (d) monohydrate at about 12% RH.

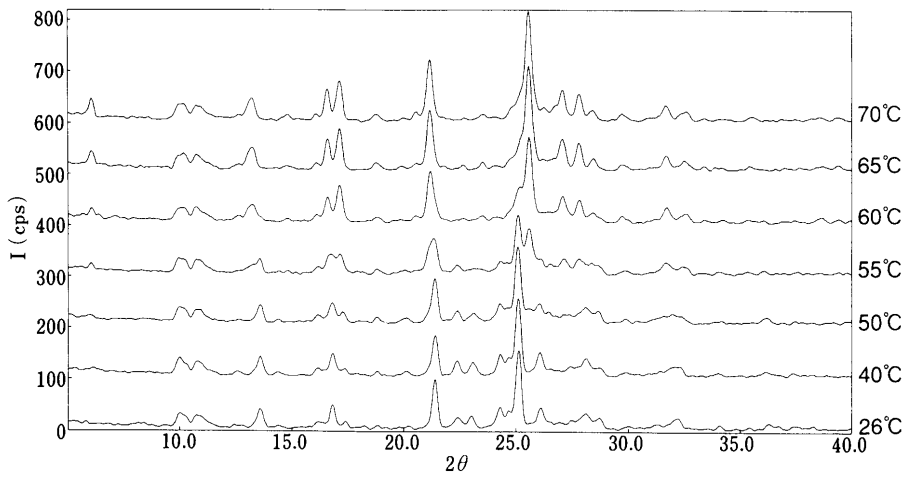


Fig. 5. Change in Powder X-Ray Diffraction Patterns of the Hemihydrate by Heating

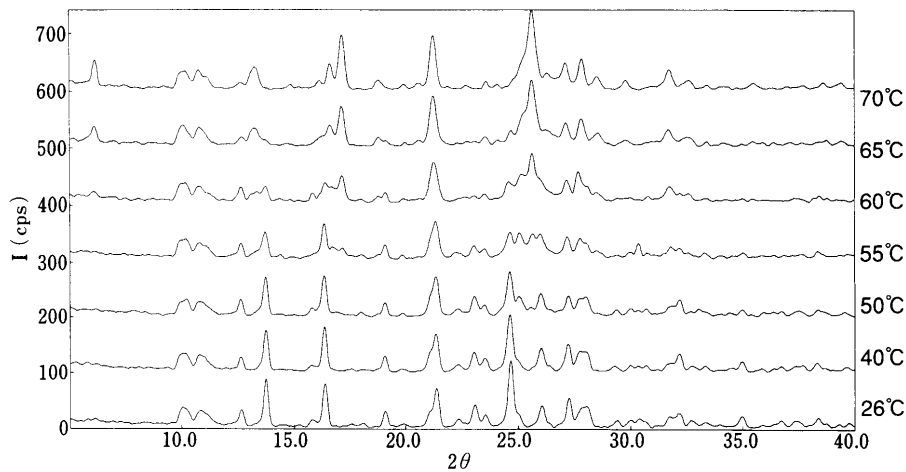


Fig. 6. Change in Powder X-Ray Diffraction Patterns of the Monohydrate by Heating

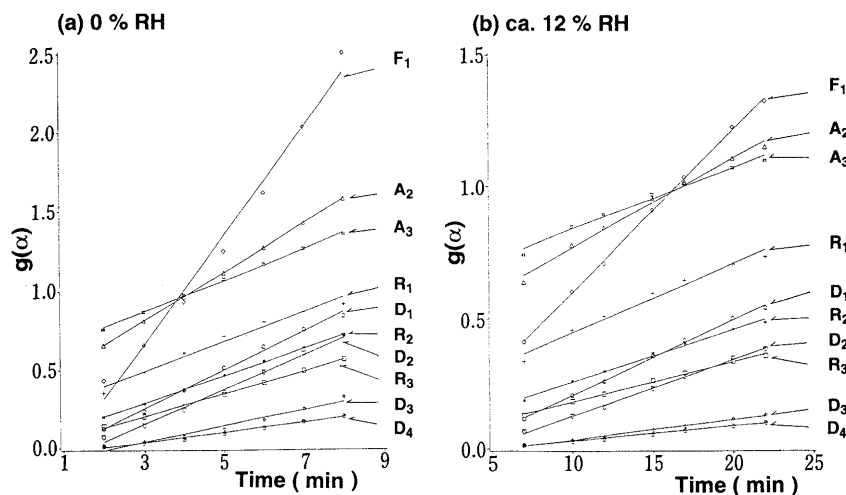


Fig. 7.  $g(\alpha)$  vs. Time Plots for the Dehydration of the Hemihydrate at 0% RH and *ca.* 12% RH at 60 °C

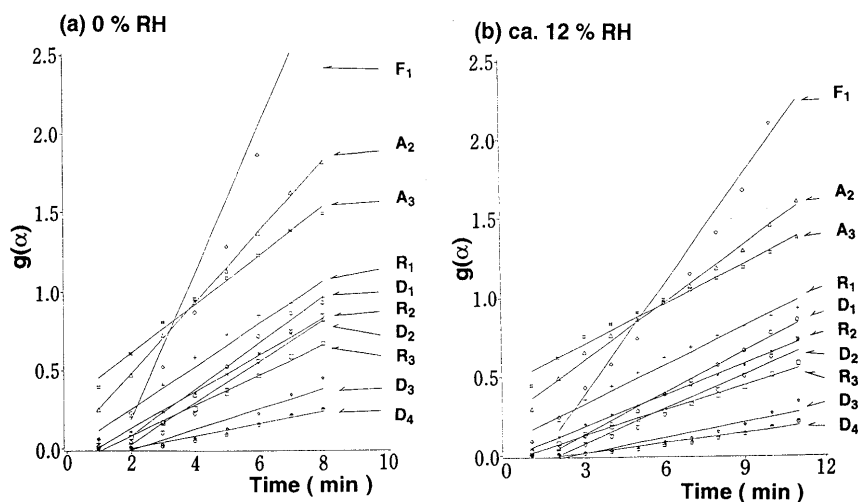


Fig. 8.  $g(\alpha)$  vs. Time Plots for the Dehydration of the Monohydrate at 0% RH and *ca.* 12% RH at 60 °C

Table 2. Rate Constants ( $k$ ), Correlation Coefficient ( $r$ ) and Mechanism for Dehydration of Nafagrel Hydrochloride Hemihydrate and Monohydrate Obtained at Various RH

$P_{H_2O}$ (Torr)	RH (%)	Temp. (°C)	Hemihydrate		Monohydrate	
			$k$ ( $\text{min}^{-1}$ )	Mechanism ( $r$ )	$k$ ( $\text{min}^{-1}$ )	Mechanism ( $r$ )
22.5	12.0	65	0.0636	A <sub>2</sub> (0.9900)	0.126	R <sub>2</sub> (0.9987)
22.5	15.1	60	0.0224	A <sub>2</sub> (0.9928)	0.0448	R <sub>2</sub> (0.9996)
17.8	9.5	65	0.0712	A <sub>2</sub> (0.9893)	0.158	R <sub>2</sub> (0.9995)
17.8	12.0	60	0.0339	A <sub>2</sub> (0.9957)	0.0664	R <sub>2</sub> (0.9994)
14.3	7.6	65	0.0767	A <sub>2</sub> (0.9998)	0.162	R <sub>2</sub> (0.9998)
14.3	9.5	60	0.0451	A <sub>2</sub> (0.9979)	0.104	R <sub>2</sub> (0.9979)
14.3	12.0	55	0.0166	A <sub>2</sub> (0.9983)	0.0365	R <sub>2</sub> (0.9991)
11.4	6.1	65	0.0876	A <sub>2</sub> (0.9938)	0.108	A <sub>2</sub> (0.9999)
11.4	7.6	60	0.0509	A <sub>2</sub> (0.9922)	0.107	R <sub>2</sub> (0.9993)
11.4	9.6	55	0.0244	A <sub>2</sub> (0.9960)	0.0567	R <sub>2</sub> (0.9984)
9.5	5.1	65	0.0964	A <sub>2</sub> (0.9929)	0.127	A <sub>2</sub> (0.9849)
9.5	6.4	60	0.0568	A <sub>2</sub> (0.9945)	0.0865	A <sub>2</sub> (0.9999)
9.5	8.0	55	0.0266	A <sub>2</sub> (0.9833)	0.0609	R <sub>2</sub> (0.9973)
4.8	2.6	65	0.148	A <sub>2</sub> (0.9943)	0.171	A <sub>2</sub> (0.9975)
4.8	3.2	60	0.0941	A <sub>2</sub> (0.9923)	0.114	A <sub>2</sub> (0.9986)
4.8	4.1	55	0.0711	A <sub>2</sub> (0.9936)	0.0830	A <sub>2</sub> (0.9850)
0	0	65	0.223	A <sub>2</sub> (0.9972)	0.319	A <sub>2</sub> (0.9989)
0	0	60	0.154	A <sub>2</sub> (0.9998)	0.225	A <sub>2</sub> (0.9997)
0	0	55	0.104	A <sub>2</sub> (0.9979)	0.176	A <sub>2</sub> (0.9986)

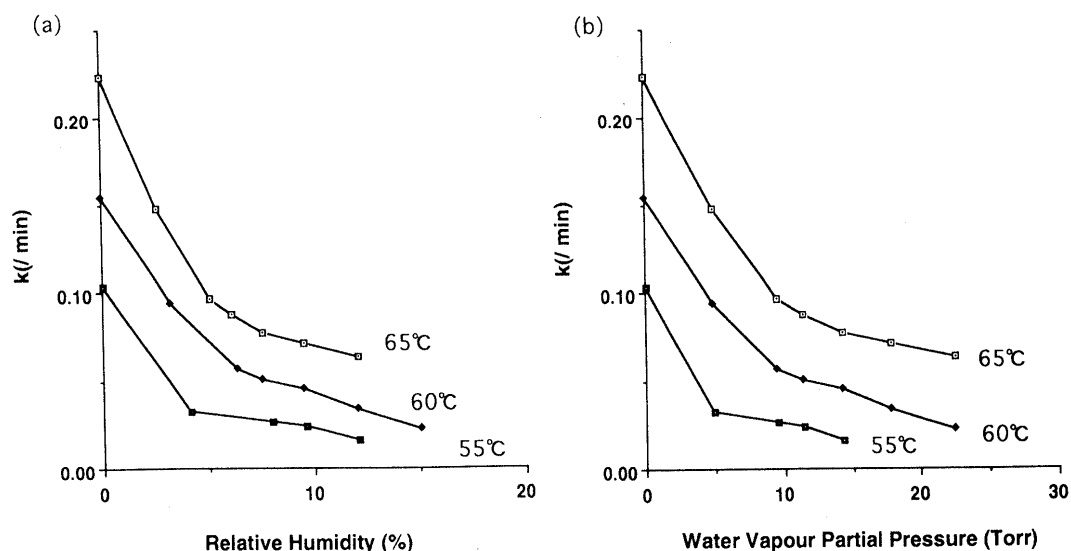


Fig. 9. Relationship between Rate Constant of Dehydration of Nafagrel Hydrochloride Hemihydrate and Relative Humidity (a), and Water Vapor Partial Pressure (b)

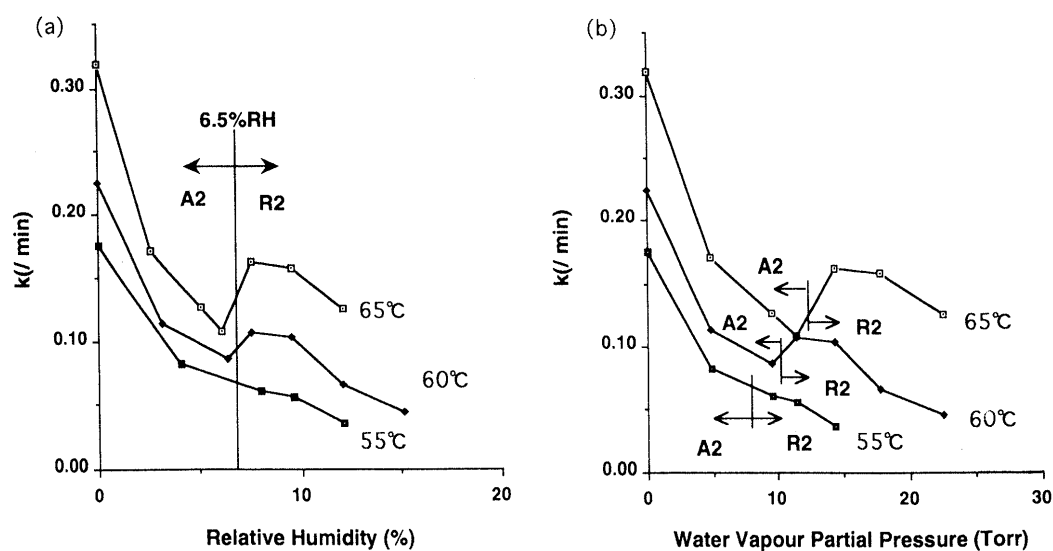


Fig. 10. Relationship between Rate Constant of Dehydration of Nafagrel Hydrochloride Monohydrate and Relative Humidity (a), and Water Vapor Partial Pressure (b)

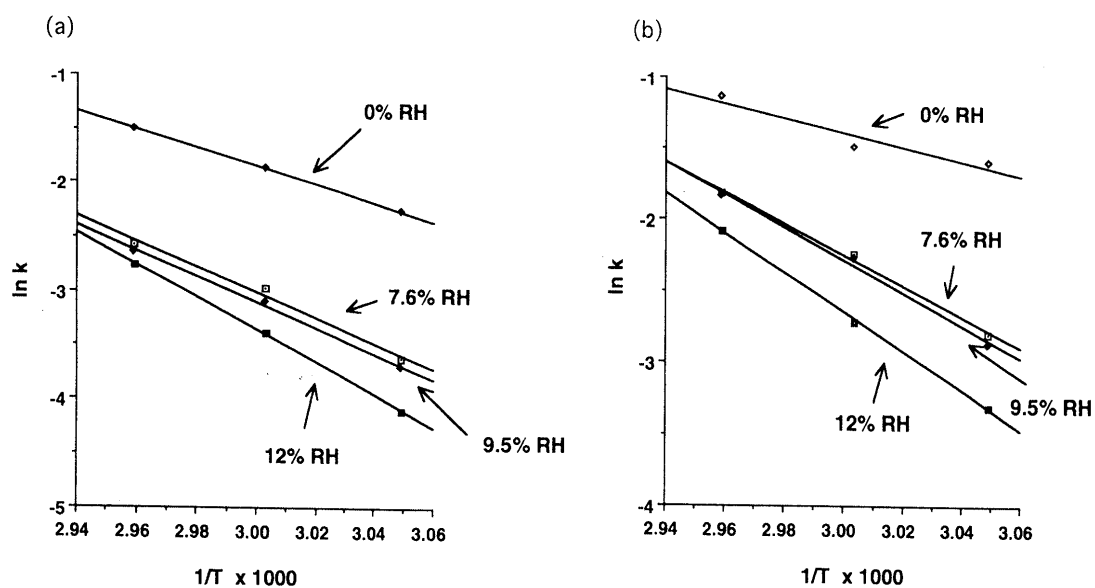


Fig. 11. Arrhenius Plots for Isothermal Dehydration of Nafagrel Hydrochloride Hemihydrate (a) and Monohydrate (b) at Various Relative Humidities

Table 3. Kinetic Parameters for Dehydration of Nafagrel Hydrochloride Hemihydrate and Monohydrate at Various RH

RH (%)	Hemihydrate→Anhydrate			Monohydrate→Hemihydrate		
	$g(\alpha)$	$E$ (kJ/mol)	$\ln A$ ( $\text{min}^{-1}$ )	$g(\alpha)$	$E$ (kJ/mol)	$\ln A$ ( $\text{min}^{-1}$ )
12	A <sub>2</sub>	124.1	41.4	R <sub>2</sub>	114.4	38.6
9.5	A <sub>2</sub>	99.0	32.6	R <sub>2</sub>	94.8	31.9
7.6	A <sub>2</sub>	98.0	32.3	R <sub>2</sub>	90.5	30.4
0	A <sub>2</sub>	70.1	23.5	A <sub>2</sub>	42.0	13.7 <sup>a)</sup>

a) Monohydrate→anhydrate.

most reliable mechanisms and correlation coefficients obtained at various RH for the dehydration of the hemihydrate and the monohydrate. All the plots give straight lines over nearly the whole range of the dehydration process. The rate constants calculated from Eq. 1 are also shown in Table 2. As seen in Table 2, the dehydration of the hemihydrate proceeded by a two-dimensional growth of the nuclei, A<sub>2</sub>, at all humidities examined.

On the other hand, although the dehydration of the monohydrate proceeded by A<sub>2</sub> at lower RH, the mechanism changed to a two-dimensional phase boundary, R<sub>2</sub>, at higher relative humidities.

Figure 9 shows the change in rate constant vs. the humidity (RH or water vapor partial pressure) for the dehydration of the hemihydrate. As Fig. 9 shows, the rate constants decreased gradually with an increase in humidity due to rehydration.

Figure 10 shows the effect of humidity on the rate constant of the monohydrate at various temperatures. The mechanism changed at about 6.5% RH, independent of the temperature, but when the rate constants were plotted against the water vapor partial pressure, the mechanism changed according to both this partial pressure (torr) and the temperature. These results indicated that the dehydration did not depend on absolute but on RH.

Activation energy,  $E$ , and the pre-exponential factor,  $A$ , were calculated from the rate constants,  $k$ , shown in Table 2. Plots of  $\ln k$  against  $1/T$  ( $T$ =absolute temperature) are shown in Fig. 11, and  $E$  and  $\ln A$  are shown in Table 3.  $E$  is strongly influenced by the RH, its value increasing as the latter rises. This phenomenon was thought to indicate that the dehydration rate decreased

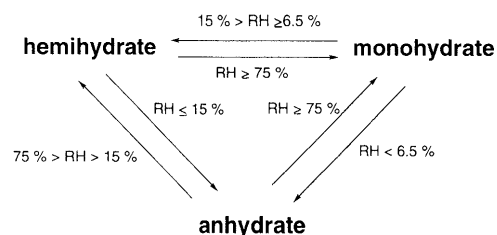


Chart 2. Possible Interconversions of Nafagrel Hydrochloride

due to the rehydration. Under all conditions, the activation energies for the hemihydrate are higher than those for the monohydrate, a finding that is consistent with a previous report<sup>3)</sup> that the monohydrate was dehydrated faster than the hemihydrate.

**Interconversion** Possible interconversions of the various phases of the drug are summarized in Chart 2. Each form was identified from its water content, powder X-ray diffraction pattern and IR spectrum. Since the hemihydrate is more stable and the monohydrate dehydrates to the hemihydrate at between 15.1% RH and 6.5% RH, we considered the mechanism of the hysteresis of the moisture equilibrium curve to be as follows: the dehydration of the monohydrate occurs at the surface of the particle and forms a hemihydrate layer on the surface. This layer hinders the elimination of the water of crystallization from the surface, thus inhibiting further conversion of the monohydrate to the hemihydrate. As a result, both hydrates were able to coexist in stable equilibrium between 23% RH and 64% RH.

#### References

- 1) Kanao M., Watanabe Y., Kimura Y., Saegusa J., Yamamoto K., Kanno H., Kanaya N., Kubo H., Ashida S., Ishikawa F., *J. Med. Chem.*, **32**, 1326 (1989).
- 2) Ball M. C., Norwood L. S., *J. Chem. Soc. (A)*, **1969**, 1633; Ball M. C., Urie R. G., *J. Chem. Soc. (A)*, **1970**, 528; Ball M. C., Casson M. J., *J. Chem. Soc., Dalton Trans.*, **1973**, 34; Sekiguchi K., Shirofani K., Sakata O., Suzuki E., *Chem. Pharm. Bull.*, **32**, 1558 (1984); Masuda Y., Nagagata K., *Thermochimica Acta*, **161**, 55 (1990).
- 3) Kitaoka H., Ohya K., *J. Thermal Anal.*, **40**, 387 (1993).
- 4) Suryanarayanan R., Mitchell A. G., *Int. J. Pharm.*, **32**, 213 (1986); Nakagawa H., Miyata T., Mohri K., Sugimoto I., Manabe H., *Yakugaku Zasshi*, **98**, 981 (1978); Yoshimatsu K., Nakabayashi S., Ogaki J., Kimura M., Horikoshi I., *ibid.*, **101**, 1143 (1981).
- 5) Sharp J. H., Brindley G. W., Achar B. N. N., *J. Am. Ceram. Soc.*, **49**, 379 (1966).